ELSEVIER

Fluorescence of 4-aminophthalimide in supercritical CO$_2$–ethanol mixtures

Diana E. Wetzler [a], Roberto Fernández-Prini [a,b], Pedro F. Aramendía [a,*]

[a] *INQUIMAE and Departamento de Química Inorgánica, Analítica y Química Física, FCEN, Universidad de Buenos Aires, Pabellón 2, Ciudad Universitaria, C1428EHA Buenos Aires, Argentina*
[b] *Unidad de Actividad Química, CNEA, Libertador 8250, 1428 Buenos Aires, Argentina*

Abstract

Steady-state and time-resolved fluorescence studies of 4-aminophthalimide (AP) in neat supercritical CO$_2$ and supercritical CO$_2$–ethanol mixtures at 35 and 45 °C are presented. In neat CO$_2$, the emission maximum of AP shifts to the red upon density increase because of the increase of average number of solvent molecules interacting with the probe. In CO$_2$–ethanol mixtures of different ethanol densities (0.025 and 0.125 M) the tendency upon CO$_2$ density increase is opposite. In mixtures, the CO$_2$ density increase, also increases the probability of exchange of the ethanol molecules interacting with AP by CO$_2$ molecules. This causes a blue shift that is bigger than the red shift caused by density increase. In all the cases, emission spectra were time independent in the nanosecond time range. This allowed to take solvation effects into account using a Langmuir adsorption model, under equilibrium conditions. This is the simplest association model that can semiquantitative describe the results and can successfully explain the lack of solvation entropic effects in emission of AP in the mixtures near the critical density of CO$_2$.
© 2004 Elsevier B.V. All rights reserved.

Keywords: 4-Aminophthalimide; Fluorescence; Solvathochromic; Supercritical fluid; Carbon dioxide; Solvation

1. Introduction

Supercritical fluids have been used intensely [1] as solvents to make static (UV and FTIR absorption [2–4], fluorescence emission [4,5], solvatochromic shifts [6–11]) and dynamic measurements (fluorescence lifetimes [11], rotational correlation times [12], vibrational energy relaxation, kinetic rate constants, specially of diffusion controlled reactions [13,14], cage effects on reactions [15–18]). The use of these fluids as solvents allows the study of solvation phenomena as a function of the density of the solvent at constant temperature. This important property of the fluid medium cannot be changed

appreciably when liquid solutions are studied far from the solvents' critical temperature.

Aminophthalimides have been extensively used as strong fluorescent probes [19–29]. 4-Aminophthalimide (AP) (Fig. 1) exhibits the common emission feature of compounds with an electron donating moiety (the amino group) and an electron acceptor moiety (one of the carbonyls of the imido group) placed in *para* position in a benzene ring. The Stokes shift of this internal charge transfer (ICT) emission is very sensitive to the polarity and hydrogen bond donating (HBD) ability of the medium. The ICT character of the transition causes a dipole moment increase upon excitation from 3.5 to 6.5 D [30]. A time dependent fluorescence spectrum was observed in neat solvents at low temperature [21,22,31] and was attributed to solvent reorientation. The same effect was also observed in solvent mixtures at higher

Fig. 1. Structure of 4-aminophthalimide.

Due to its big solvent dependent spectral shift, AP is ideal for monitoring solvation changes, specially in a mixture of a polar and a non-polar component. In this work, we present steady-state and time-resolved fluorescence studies of AP in neat supercritical CO_2 and in mixtures of ethanol and supercritical CO_2. Measurements were performed at two temperatures at different CO_2 densities.
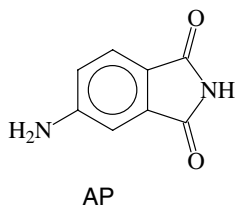
temperatures [21,32], including measurements in supercritical CO_2–2-propanol mixtures [28].

To describe solvation different models have been proposed in literature. In neat solvents, Rapp et al. [33] developed a kinetic scheme to describe the time-dependent spectral shift by stepwise reorientation of solvent molecules in the solvation sphere. This model leads to Bakhshiev's formula [19,34] for the dependence of the mean energy of the emission with time, which is monoexponential.

For solvent mixtures, Suppan [29,35] took into account the different interaction energy of the solute with the solvent mixture components using a continuum dielectric approach. He introduced the concept of dielectric enrichment to describe the concentration enhancement of the more polar component of the solvent mixture in the vicinity of a polar solute, i.e. the phenomenon of preferential solvation. In a previous work [32], we presented a kinetic scheme to describe the exchange of solvent molecules and the time-dependent fluorescence emission spectra of AP in toluene–ethanol mixtures based on a Langmuir type association of solvent molecules with the solute. A similar analysis using a quenching model, developed by Moore et al. [36], was applied to aminonaphthalimide derivatives in aqueous-ethanolic solutions [37].

It is known that solvation in supercritical pure fluids close to the critical temperature of the solvent entails the phenomenon of local density enhancement, i.e. the solvent close to the attractive solute shows inhomogeneities leading to an increase of its local density. This characteristic has been found experimentally [38–40] and proven theoretically [41–43] and by simulation studies. Kajimoto et al. [44] and Otomo and Koda [40] could explain the solvation characteristics of probes in supercritical fluids using a Langmuir adsorption model. In supercritical solvent mixtures preferential solvation is present as in dense fluids mixtures, the composition of the solvent component with bigger interactions is larger close to the solute. Due to the lower fraction of the total volume occupied by solvent molecules, composition differences between the first solvation sphere and bulk are bigger and diffusion processes are faster than in normal dense fluids. The composition of the solvent in the first solvation sphere will be very dependent on pressure.

2. Experimental

AP (Acros Organics) 97% was recrystallized from ethanol. Solvents: ethanol 95% v/v azeotropic mixture with water (the use of this reagent instead of pure ethanol permitted to have a constant H_2O–ethanol ratio in all the mixtures, its possible influence in the spectral shifts is discussed below) (Merck, for spectroscopy) and carbon dioxide (AGA, Coleman 99%) were used as received.

A typical experimental setup to measure with supercritical fluids was used as described previously [45]. A high-pressure optical cell made of stainless steel was used to perform all the measurements. It was equipped with three sapphire windows of 10 mm thickness. The equipment included a high-pressure hand-operated pump and a six-port valve.

Corrected fluorescence emission and excitation spectra were recorded under steady-state conditions in a PTI-Quantamaster apparatus. Spectra were obtained at two different temperatures: 35 and 45 °C as a function of CO_2 density. Time-resolved fluorescence decays were measured in a fluorescence lifetime spectrometer (PTI-Time Master). Decay curves were recorded at different emission wavelengths.

Temperature was controlled by external water circulation and measured in the cell with a ceramic thermistor calibrated against a standardized Beckman thermometer (precision 0.005 K), to within 0.05 K. Pressure was measured with a pressure transducer (Burster), calibrated against a deadweight gauge (Ruska; precision 0.01%). The calibration was verified measuring the vapor pressure of ethane as a function of temperature in the 300–305 K range [45].

Depending on the solvent used, neat CO_2 or CO_2–ethanol mixtures, two different methods to introduce the sample in the cell were employed. In the case of neat CO_2, a little amount of solid AP was placed in the cell and then the fluid was introduced up to a pre-selected pressure. After each addition of CO_2 steady-state emission spectra were recorded. The same method was employed at both temperatures. Published equation of state for CO_2 [46] was used to obtain the molar density of the fluid from experimental values of pressure and temperature.

For CO_2–ethanol mixtures a different method was used to prepare the solutions. The CO_2–ethanol mixtures were prepared inside the high-pressure cell. A known volume of ethanol containing a little amount of AP was introduced in the cell through the six-port valve using a calibrated capillary tube. The thermostated pressure transducer chamber was used to evaluate the amount of CO_2 before adding it to the high-pressure cell. The transducer volume was determined previously, thus, making use of p–T–V data and a published equation of state [46], the number of CO_2 moles that were added to the high-pressure cell could be determined. The molar density of CO_2 in each mixture could be accurately calculated using the volume of the high-pressure cell. The emission spectrum was recorded at both temperatures (35 and 45 °C) before adding a new amount of CO_2 to the cell. In order to work at two different densities of ethanol (0.025 and 0.125 M), we repeated this procedure using two different capillary loops to add this solvent. The molar fraction of ethanol was always kept smaller than 0.02, in order to have only one fluid phase [47–49].

3. Results

Fig. 2 shows the normalized steady-state emission spectra of AP in a series of CO_2–ethanol mixtures. It can be seen that emission spectra shift to the red as the ethanol mole fraction in the mixture increases. Similar results were observed in liquid mixtures [21,32] and in supercritical CO_2–2-propanol mixtures [28].

Fig. 3 shows the emission maximum shift with respect to the value in *n*-hexane (see below) of AP in different supercritical mixtures. In neat CO_2, the
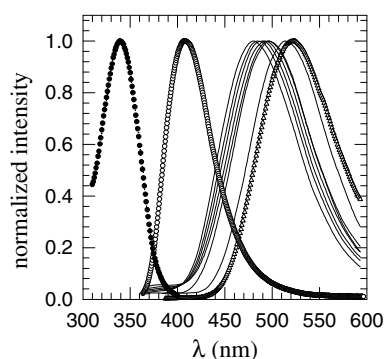

Fig. 3. Emission spectral shift as a function of CO_2 density. (a) Neat CO_2. (b) Neat CO_2 and CO_2–ethanol mixtures. Symbols: experimental data. Lines: fit to Eqs. (3) or (4). Full symbols: 35 °C and open symbols: 45 °C. Circles: neat CO_2, triangles: CO_2–ethanol mixtures of $\rho_{eth} = 0.025$ M, squares: CO_2–ethanol mixtures of $\rho_{eth} = 0.125$ M.

maximum of emission shifts to the red as density increases because of the increase of the average number of solvent molecules interacting with the probe. In CO_2–ethanol mixtures of different ethanol densities (0.025 and 0.125 M) the tendency upon a CO_2 density increase is opposite. This can be explained taking into account that as CO_2 density increases, the probability of exchange of ethanol molecules by CO_2 molecules interacting with AP, also increases, i.e. ethanol is displaced by the increasing density of CO_2. This causes a blue shift that is bigger than the red shift caused by the density increase.

In both cases, a thermochromic effect can be observed. Emission spectra shift to the blue upon temperature increase. The same effect was observed for AP in toluene–ethanol and toluene–acetonitrile mixtures [32].

In neat CO_2 and in the CO_2–ethanol mixtures studied in this work, emission spectra were time independent in the nanosecond time range. These results differ from the result found in CO_2–2-propanol [28] and toluene–ethanol [32] mixture where emission spectra shift to the red as a function of time in the nano- or subnanosecond

Fig. 2. Peak-normalized corrected steady-state emission spectra of AP in supercritical CO_2–ethanol mixtures at different density of CO_2 and at fixed $\rho_{eth} = 0.125$ M. Emission spectra in neat solvents at the same temperature are shown: (○) neat CO_2, $\rho_{CO_2} = 20.1$ M and (△) neat ethanol. Fluorescence excitation spectrum in neat CO_2, $\rho_{CO_2} = 20.1$ M, is shown as the leftmost curve (●). All the spectra were recorded at 35 °C. The CO_2 molar density of mixtures is, from left to right, 18.4, 16.9, 15.5, 14.2, 12.3, 10.6, 8.3 M.
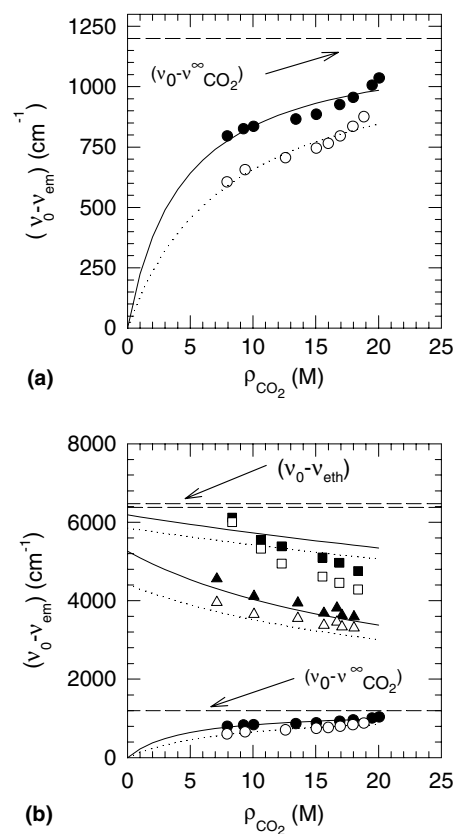
Table 1
Lifetimes for total fluorescence decay obtained by a global analysis of the data at different emission wavelengths at each temperature and composition

T (°C)	ρ_{CO_2} (M)	ρ_{eth} (M)	(%mol/mol)$_{eth}$	τ (ns)
35	7.1	0.000	0.00	6.0
35	12.8	0.000	0.00	9.9
35	15.4	0.000	0.00	11.9
35	18.0	0.025	0.13	9.5
35	14.9	0.025	0.18	16.0
35	10.4	0.025	0.24	20.0
35	7.4	0.025	0.34	19.8
35	15.1	0.125	0.82	15.0
35	10.5	0.125	1.18	19.5
35	7.8	0.125	1.57	20.7
45	15.4	0.000	0.00	9.0
45	18.0	0.025	0.13	9.1

time range. In the mixtures studied in this work, the expected time dependence of the emission spectra might fall in the subnanosecond or picosecond time domain, faster than the time resolution of our experiment. All the fluorescence decays, monitored at different emission wavelengths, can be fitted by a monoexponential function with the same lifetime for a given temperature and CO$_2$ and ethanol densities (see Table 1).

If we wish to use a model to describe solvation, we have to consider that the solvation shell of AP in the excited state (AP*) can accommodate a limited number of solvent molecules. Besides, when the number of solvent molecules attached to the probe increases, the accommodation of a new molecule of solvent becomes more difficult. The simplest way to take these effects into account is by the use of a Langmuir adsorption model. This model was used to describe solute–solvent association in supercritical fluids in a variety of systems by different authors. Kajimoto [44] used it in his study of the density dependent emission of 4-(N,N-dimethylamino)benzonitrile in fluoroform. A Langmuir adsorption based model, called by the authors a concentric shell model, was also used to describe the solvation of ions of the Groups 1, 2, and 17 in supercritical water [50]. This approach predicted free energies of solvation which agreed with molecular simulation. Also Otomo and Koda [40] successfully used the Langmuir model derived by Kajimoto to analyze the solvent density dependent spectral shifts of benzene, chlorobenzene, anthracene, 2-nitroanisole, 4-aminobenzophenone, and 4-(N,N-dimethylamino)benzonitrile in supercritical CO$_2$. Good descriptions were obtained for solutes with similar characteristics as 4-AP (as 4-(N,N-dimethylamino)benzonitrile and 4-aminobenzophenone) in polar and in non-dipolar solvents. As the simplest association model, it cannot account quantitatively in a quite satisfactory way for the solvatochromic features of the system in the whole concentration range studied. Yet it yields reasonable explanations for the trends observed in the sol-

vation as discussed below and can be taken as a reference to explain the deviations.

The use of Langmuir model to describe solvation in neat CO$_2$, under equilibrium conditions, derives the following equation:

$$\langle n \rangle = m \frac{K_{CO_2}\rho_{CO_2}}{1 + K_{CO_2}\rho_{CO_2}}, \tag{1}$$

where $\langle n \rangle$ is the average number of molecules in the solvation shell of AP*, m is the maximum number of molecules that can be accommodated, ρ_{CO_2} is the bulk molar density of CO$_2$ and K_{CO_2} is the association equilibrium constant between AP* and CO$_2$.

If we assume that each solvent molecule in the first solvation sphere has the same contribution to the spectral shift, Δv, the free energy difference (measured as wavenumber) between the emission in vacuum and in the solvent, can be written as a linear function of $\langle n \rangle$:

$$\Delta v = \frac{\left(v_0 - v_{CO_2}^\infty\right)}{m} \langle n \rangle, \tag{2}$$

where $\Delta v = v_0 - v_n$ and v_n, v_0 and $v_{CO_2}^\infty$ are the wavenumbers of the maximum of fluorescence emission of AP at each density, in the vacuum, and at high density of CO$_2$, respectively. Eq. (2) is consistent with the assumptions made to derive the Langmuir model for association and the usual spectroscopic assumption that the 00 band of a species is an average of the maxima of absorption and emission [51]. Using Eq. (1), we can rewrite Eq. (2), as:

$$\Delta v = \left(v_0 - v_{CO_2}^\infty\right) \frac{K_{CO_2}\rho_{CO_2}}{1 + K_{CO_2}\rho_{CO_2}}. \tag{3}$$

The value of $v_{CO_2}^\infty$ and K_{CO_2} are the fitting parameters in Eq. (3). The value of the emission maximum in n-hexane (25,575 cm^{-1}) was used for v_0 because the value in vacuum was not available and we did not wish to introduce a new fitting parameter.

The validity of this approximation can be supported if we take into account that the magnitude of the absorption shift in different solvents is small and that the Stokes shift for AP in vacuum (5000 cm^{-1}) [20] is very similar to the Stokes shift in n-hexane (4714 cm^{-1}). This later value is calculated using the linear correlation between the Stokes shift of AP and E_T (30) that was found in neat solvents [32,52,53]. For the parent compound, 4-amino-N-methylphthalimide, the absorption shift between the vapor [54] and toluene is negligible (the two are at $\lambda_{abs} = 356$ nm).

The results of the fit of the data to Eq. (3) for two isotherms are summarized in Table 2 and plotted in Fig. 3(a).

A similar analysis can be made for the data obtained in CO$_2$–ethanol mixtures. In this case a competitive Langmuir adsorption model can be used. The spectral shift, assumed to be additive, can be written in the following way:

Table 2
Values of K_{CO_2} and $v^\infty_{CO_2}$ obtained by fitting spectral shifts in neat CO_2 to Eq. (3)

T (°C)	K_{CO_2} (M^{-1})[a]	$v^\infty_{CO_2}$ (cm^{-1})
35	0.23	24,375
45	0.13	24,392

[a] Errors ±30%.

$$\Delta v = \left(v_0 - v^\infty_{CO_2}\right) \frac{K_{CO_2}\rho_{CO_2}}{1 + K_{CO_2}\rho_{CO_2} + K_{eth}\rho_{eth}}$$
$$+ \left(v_0 - v_{eth}\right) \frac{K_{eth}\rho_{eth}}{1 + K_{CO_2}\rho_{CO_2} + K_{eth}\rho_{eth}}, \quad (4)$$

where v_{eth} is the wavenumber of the maximum of fluorescence of AP in neat ethanol (at the same temperature), K_{eth} is the association equilibrium constant between AP* and ethanol and ρ_{eth} is the molar density of ethanol in the mixture. We applied this model to the spectral shift data in neat CO_2 and two mixtures of CO_2–ethanol ($\rho_{eth}=0.025$ and 0.125 M). In Eq. (4) K_{eth} is the adjustable parameter. The values of the other parameters: v_0, $v^\infty_{CO_2}$ and K_{CO_2} were taken equal to those in neat CO_2, and v_{eth} was taken from the emission spectrum in ethanol (see Table 3). The latter two were obtained from the fit of the data of Fig. 3(a) to Eq. (3). Results are shown in Table 3 and in Fig. 3(b). Eqs. (1), (3), and (4) assume that ρ_{eth} and ρ_{CO_2} are a good measure of their activity. Due to the dilute range in ethanol concentration, we can assume that we work within the very dilute limit, and therefore formally include the constant infinite dilution activity coefficient in the calculated K_{eth}. On the other hand, we can consider CO_2 as a pure solvent in all the conditions of our experiments, and therefore its concentration should coincide with its activity.

4. Discussion

The fluorescence decay of AP is monoexponential in all cases studied in this work and we do not observe any spectral shift with time in the nanosecond time range. These two observations point to the fact that the expected diffusion controlled solvent exchange in the solvation sphere of AP* takes place in the subnanosecond scale, below the time resolution of our experiment. Betts and Bright [28] observed spectral shifts to the red in time-resolved emission spectra and a biexponential fluorescence decay for 4-amino-N-methylphthalimide in CO_2–2-propanol mixtures at 45 °C, 136 bar total pressure and mole fraction of 2-propanol (x_{prop}) between 0.50% and 2.00%. The shorter lifetime observed by them decreases with the increase of x_{prop} from 1.22 ns at $x_{prop}=0.50\%$ to 0.65 ns at $x_{prop}=2.00\%$. They interpreted this observation as the formation of a solute–solvent complex. Nevertheless, a diffusion controlled exchange of CO_2 by alcohol in the solvation sphere would have the same consequence. Our observations are compatible with those of Betts and Bright [28] if the exchange of ethanol for CO_2 is faster than the exchange of 2-propanol, causing the exchange to be completed within 1 ns. This is possible since most of our experiments were performed at lower pressure, were diffusion is expected to be faster. We consider that the differences observed cannot be caused by the use of the N-methyl derivative of AP, due to the quite similar behavior observed for both probes [32].

The above discussion leads to the conclusion that the fluorescence decay observed takes place in an equilibrated excited state with respect to solvation, thus supporting the application of an equilibrium model, as the one depicted by Eq. (4).

The lifetimes in Table 1 show an increase with alcohol mole fraction. This fact is in agreement with the behavior of the longer lifetime reported in the above referenced work [28], as well as with observations performed in supersonic jets of AP and AP–water clusters [29]. The emission lifetime also increases with the solvent concentration in neat CO_2. On the other hand, it is known that the excited state lifetime of AP* in protic solvents is shorter than in aprotic ones and that the emission quantum yield also decreases drastically [24,26,37]. The above facts lead to the conclusion that there are two opposite effects of ethanol in the deactivation pathways of the excited state. The emission of

Table 3
Values of K_{eth} obtained by fitting spectral shifts in neat CO_2 and in CO_2–ethanol mixtures to Eq. (4)

T (°C)	v_0 (cm^{-1})[a,c]	$v^\infty_{CO_2}$ (cm^{-1})[a,d]	v_{eth} (cm^{-1})[a,e]	K_{CO_2} (M^{-1})[a,d]	K_{eth} (M^{-1})[b]
35	25,575	24,375	19,100	0.23	173
45	25,575	24,392	19,200	0.13	90

The values of the constant parameters used to fit the data are also presented in this table.
[a] Constant parameters.
[b] Fitting parameters (errors ±10%).
[c] Emission maximum in n-hexane (see Section 3).
[d] Obtained from the fit of the spectral shift in neat CO_2 to Eq. (3) (see Table 2).
[e] From [32].

AP* is originated in an excited state that has an ICT character and a relaxed geometry that makes the amino group coplanar with the aromatic ring [21,32]. The ICT character of the excited state is enhanced by interaction with the solvent and the accompanying change in geometry with respect to the ground state imposes a nuclear barrier to the radiative and non-radiative transition to the ground state. This explains the excited state lifetime increase in CO_2 and at low concentrations of ethanol. The excited state of AP has also an enhanced H-bond acceptor capacity. The deactivation pathway provided by H-bonding is responsible for the lifetime decrease in protic solvents with respect to aprotic ones. If we take into account the values of the fluorescence quantum yield (ϕ_f) and the fluorescence decay time (τ_f) in dioxane ($\phi_f = 0.72$ and $\tau_f = 15$ ns) and in methanol ($\phi_f = 0.10$ and $\tau_f = 6.9$ ns) [24] and we write the fluorescence decay rate ($1/\tau_f$) as the sum of the radiative (k_r), and non-radiative (k_{nr}) rate constants of AP*, then $1/\tau_f = k_r + k_{nr}$. In this way, we can calculate that k_r drops from 4.9×10^7 s^{-1} in dioxane to 1.45×10^7 s^{-1} in methanol. On the other hand, k_{nr}, increases from 1.8×10^7 s^{-1} in dioxane to 1.3×10^8 s^{-1} in methanol. In conclusion, at very low alcohol concentrations, the effect of the geometry difference predominates, and an increase in the excited state lifetime is observed. At higher alcohol concentration, the effect of H-bonding decreases both ϕ_f and τ_f.

Solvatochromic shifts were described by a dielectric enrichment model by Suppan and co-workers [30,35]. The theory of Suppan points mainly to non-specific electrostatic interactions. This system has a strong component of H-bond interactions [21,31,32,35] and therefore is not the best suited to test our model for CO_2–ethanol mixtures. Dipolar interactions, certainly, play a role, but H-bond interactions are also very important here. By applying his approach of dielectric enrichment, Suppan points out that the emission of AP shows anomalous behavior in protic solvents whereas absorption does not [35]. This is the reason why we preferred to use the association model rather than the dielectric enrichment model of Suppan.

The fit to the Langmuir model adopted here is particularly poor at the higher ethanol concentration. The deviations are larger than the uncertainty in the Stokes shifts (typically ± 100 cm^{-1}). As ethanol has a much bigger affinity for AP than CO_2 it is possible that under the analyzed conditions, aggregation of AP and ethanol occurs, rendering the environment surrounding the AP molecule in its excited state more similar to neat ethanol than would be expected. These aggregates are broken when ρ_{CO_2} increases and the spectral shifts would change more strongly with ρ_{CO_2}. The use of a more refined model would require to have more measurements, specially in the low ρ_{CO_2} region. However, measurements in that concentration range were not suitable for spec-
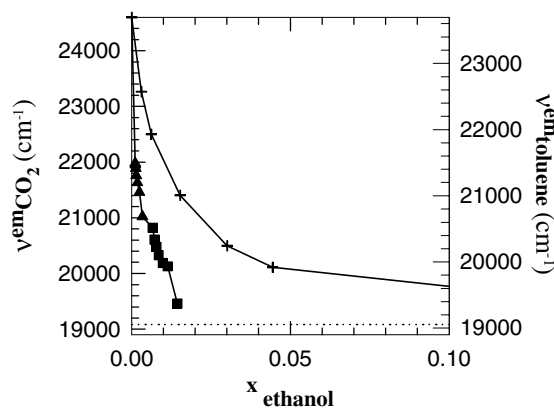

Fig. 4. Maximum emission wavelength at 35 °C as function of ethanol molar fraction in CO_2–ethanol (triangles: CO_2–ethanol mixtures of $\rho_{eth} = 0.025$ M, squares: CO_2–ethanol mixtures of $\rho_{eth} = 0.125$ M) and in toluene–ethanol mixtures (crosses).

tral analysis due to the high noise associated to the low solubility of AP.

The mole fraction of EtOH 95% v/v does not exceed 1.5% mol/mol (see Fig. 4), therefore the mole fraction of water in the total system is not exceeding 0.2%. We do not expect this small amount of water will have any decisive influence on the solvation data. On one side, there is a very small difference between the solvation ability of water and that of ethanol for AP or AP* (the emission maxima are 524 nm for ethanol and 540 for water [24], against 408 nm for CO_2), $E_T(30)$ scale shows a similar behavior [52]. So, the difference between either of these H-bond donating solvents and CO_2 is much bigger than it is between them. We measured less than 2 nm difference in the emission maximum of AP in absolute EtOH and EtOH 95% v/v in water. Even though one may argue that the molar amount of water highly exceeds the molar amount of AP, there is no evidence, even in liquid EtOH 95%, that this proportion of water has an appreciably greater influence in the solvation as compared to EtOH. We additionally do not observe a time dependent shift in the emission spectrum that might account for influence of the water molecules in the solvation of AP* (diffusion of the more diluted water component will take place in a slower time domain and is expected to fall in the time window of observation in the nanosecond range). On the other side, given the mole ratio of 7:1 ethanol:water, and the occupancy numbers (vide supra), the average number of water molecule in the solvation sphere should be smaller than one.

A thermodynamic analysis can be made in order to interpret the model proposed in this work for the solvent induced spectral shift (Eq. (4)). The following equation can be written making a thermodynamic cycle of free energy (see Scheme 1):

$$\Delta F_{abs} + \Delta F_{rel,e} + \Delta F_{em} + \Delta F_{rel,g} = 0, \tag{5}$$

where ΔF_{abs}, ΔF_{em} are the free energy of absorption and emission and $\Delta F_{rel,e}$, $\Delta F_{rel,g}$ are the free energies associated to the relaxation from the Franck–Condon states to the equilibrated states in the excited and ground electronic surfaces, respectively.

The relaxation free energies can be separated in two contributions:

$$\Delta F_{rel,j} = \Delta F_{rel,j}^{\varepsilon_0} + \Delta F_{rel,j}^{sv}, \tag{6}$$

where the first term is the ΔF of relaxation in the vacuum and the second one is due to solvent and probe reorganization. These two contributions to solvation are often referred to as inner and outer sphere reorganization, respectively. In Eq. (6), the subscript $j=e$ refers to excited state reorganization energy, and $j=g$ refers to ground state reorganization.

Using Eqs. (5) and (6), ΔF_{em} can be written in the following way:

$$\Delta F_{em} = (-\Delta F_{abs} - \Delta F_{rel,e}^{\varepsilon_0} - \Delta F_{rel,g}^{\varepsilon_0}) - (\Delta F_{rel,e}^{sv} + \Delta F_{rel,g}^{sv}). \tag{7}$$

The solvatochromic shift in absorption is much smaller than in emission for 4-AP [35], so in the concentration range of our measurements, we can assume that ΔF_{abs} is independent of the medium. This assumption is further based upon the fact that the excitation maximum in CO_2 (Fig. 2) is very near the absorption maximum in toluene or toluene ethanol-mixtures of $x_{ethanol} < 0.01$ [32]. Under this assumption, the first term between brackets in Eq. (7) is equal to the free energy of emission in vacuum ($\Delta F_{em}^{\varepsilon_0}$) and Eq. (7) can be re-written as:

$$\Delta F_{em} = \Delta F_{em}^{\varepsilon_0} - (\Delta F_{rel,e}^{sv} + \Delta F_{rel,g}^{sv}). \tag{8}$$

The model that is described by Eq. (4) to account for the solvent effect, can be re-written in terms of free energy in the following way:

$$\Delta F_{em} = \Delta F_{em}^{\varepsilon_0} - N_A \overline{\Delta F}_{CO_2} \langle n \rangle_{CO_2} - N_A \overline{\Delta F}_{eth} \langle n \rangle_{eth}, \tag{9}$$
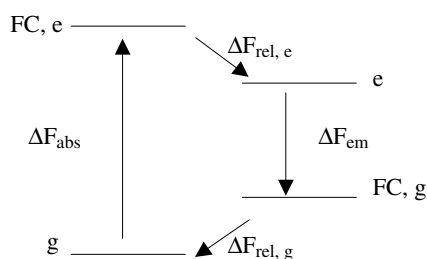
Scheme 1. Thermodynamic cycle. ΔF_{abs}, ΔF_{em} are the free energy of absorption and emission and $\Delta F_{rel,e}$, $\Delta F_{rel,g}$ are the free energies associated to the relaxation from the Franck–Condon states to the equilibrated states in the excited and ground electronic surfaces, respectively. g: relaxed ground state; FC,e: Franck–Condon excited state; e: relaxed excited state; FC,g: Franck–Condon ground state.

where N_A is the Avogadro's number and $\overline{\Delta F}_{CO_2}$ and $\overline{\Delta F}_{eth}$ are the contributions to the shift in ΔF_{em} relative to vacuum per molecule of CO_2 and ethanol in the solvation sphere, respectively.

Comparing Eq. (8) with Eq. (9), we can write the solvent contribution to the relaxation free energy in terms of the model:

$$\Delta F_{rel,e}^{sv} + \Delta F_{rel,g}^{sv} = N_A (\overline{\Delta F}_{CO_2} \langle n \rangle_{CO_2} + \overline{\Delta F}_{eth} \langle n \rangle_{eth}). \tag{10}$$

Eq. (10) reflects the known fact that the free energy change measured by the Stokes shift contains contributions from the excited and ground state relaxations. If the equilibrium configurations in the two electronic surfaces have a great difference, then the same factors that contribute to the relaxation of the excited state, increase the free energy of the ground state (see Scheme 1). Consequently, the decrease in the free energy of emission caused by each additional solvating molecule is greater than the free energy of interaction with the excited state.

We will comment briefly on the temperature influence in the solvation state. The association of CO_2 and ethanol with AP* are both exothermic, as expected and as reflected in the decrease of the association equilibrium constants with temperature, for both CO_2 and ethanol (see Table 3). The values of the internal energy difference, ΔU, derived from the temperature dependence of K_{CO_2} and K_{eth} are −46 and −53 kJ/mol. The error of these ΔU values are greater than 50% due to the limited temperature range measured and to the relatively big errors in the individual values of the association equilibrium constants. Nevertheless, these values are greater than expected for a dipolar interaction plus a H-bond interaction but this is expected considering the discussion of the previous paragraph.

Fig. 4 shows a plot of the maximum emission wavelength versus the mole fraction of ethanol in mixtures with CO_2 as well as the data for mixtures with toluene [32]. The more pronounced variation of emission maximum in the case of CO_2–ethanol mixture indicates that ethanol replaces CO_2 more easily than toluene. This conclusion is in line with the lower solvation interaction of CO_2 compared to toluene and evidenced in the lower Stokes shift (4900 cm^{-1} in CO_2 and 4930 cm^{-1} in toluene) and lower emission maximum (408 nm in CO_2 and 423 nm in toluene). To measure the magnitude of this trend, we must compare the equilibrium constants we obtained in this work (see Table 3) with the results we had obtained in toluene–ethanol mixtures. In our previous work we measured the kinetic exchange constants between a molecule of toluene and a molecule of ethanol in the sphere of solvation of AP*, so we can calculate the equilibrium exchange constant between these two solvents:

AP^*–toluene + ethanol ↔ AP^*–ethanol + toluene
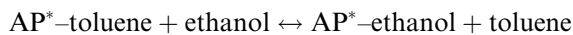
$$K_{toluene\rightarrow ethanol}^{35\,°C} = 10$$

In this work, as we employed a supercritical fluid as a solvent instead of a typical liquid we obtained the individual association equilibrium constant for CO_2 and for ethanol:

$AP^* + CO_2 ↔ AP^*$–CO_2 K_{CO_2}

$AP^* + ethanol ↔ AP^*$–ethanol K_{eth}
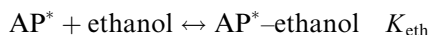
In order to compare both systems, we calculated the exchange equilibrium constant between CO_2 and ethanol, $K_{CO_2\rightarrow ethanol}^{35\,°C} = K_{eth}/K_{CO_2} = 752$. As CO_2–ethanol exchange equilibrium constant is bigger than the constant for toluene–ethanol system, we can conclude that solvating CO_2 molecules are more easily replaced by ethanol, than toluene molecules. This conclusion is strictly valid for infinitely diluted ethanol in toluene or CO_2 and depends on the free energy difference of transfer of ethanol at infinite dilution between these two solvents. We do not think that this contribution is so large as to change the conclusion, considering that the spectroscopic evidence also points in the same direction. There are in principle two contributions that explain the lower solvation capacity of CO_2 with respect to toluene. First, the greater interaction of toluene with the aromatic portion of AP, and second a more negative entropic contribution to solvation in CO_2–ethanol mixtures. This latter arises not only in the fact that the bulk has a different composition than the solvation sphere (which is enriched in the more polar component), but also because supercritical CO_2–ethanol mixtures are expanded fluids. The second contribution is not present in the case of dense liquids like toluene–ethanol mixtures.

In what follows, we will estimate the relative importance of these two contributions, by comparing entropic effects in CO_2–ethanol to toluene–ethanol mixtures. We can extract model-free thermodynamic conclusions from the variation of Δv with temperature at constant bulk composition and volume. This thermochromic shift amounts to 100 cm^{-1} for CO_2 and 250 cm^{-1} for CO_2–ethanol mixtures (as average in the concentration range), between 35 and 45 °C.

In spite of the fact that the Franck–Condon approximation implies that the atomic nuclei have the same configuration in the excited and ground state when emisson occurs, there is an entropic contribution due to the difference of density of states before and after emission. This is supported by the thermochromic effect and the fact that in binary solvent mixtures the effect of temperature is much larger than in the pure solvents [30,32].

So, if we interpret the thermochromic shift as the entropy change associated to the emission (ΔS_{em}), these

values are: 120 J K^{-1} mol^{-1} for CO_2 and 300 J K^{-1} mol^{-1} for the mixtures. In all the cases, the values are positive because of the ordering effect of the more polar excited state. In the later case, the contribution to entropy is greater, due to the composition change in the solvation sphere. Suppan [30] finds similar effects for the emission of 4,4′-dimethylaminonitrostilbene in cyclohexane–tetrahydrofurane mixtures. The values of ΔS_{em} in toluene–ethanol mixtures are between 350 and 400 J K^{-1} mol^{-1} in the 0.025–0.125 M ethanol concentration range [32]. If we compare them to the above quoted value in CO_2–ethanol we can conclude that the compressibility of the fluid does not contribute appreciably to ΔS_{em}.

The fit to the solvation data is independent of the value of m, the maximum number of solvating molecules. To estimate m we need additional data. We can take this number as 8 ± 1, as determined for ethanol and toluene from kinetic and thermodynamic analysis [32]. Taking this into account, we can calculate, for example, that in neat CO_2: AP^* interacts with six CO_2 molecules at the critical density (10.6 M) at 35 °C and with five at the same density and 45 °C. When 0.025 M ethanol is added at 35 °C, the average number of solvent molecules interacting with AP^* is five for ethanol and three for CO_2. As a comparison, in toluene–ethanol mixtures with 0.025 M ethanol at 27 °C, AP^* is solvated by two molecules of ethanol and six molecules of toluene. From the previous data we can conclude that in supercritical mixtures, ethanol not only displaces CO_2 molecules but also fills empty solvation positions. The sphere is almost completely occupied. This fact also points to a very mild compressibility contribution to ΔS_{em}.

The occupation numbers derived in the preceding paragraph are dependent on the parameters obtained by the application of the Langmuir model, which has limitations in accuracy at the higher ethanol concentrations. Nevertheless, similar conclusions can be attained independently based on inspection of Fig. 3. At the critical density, the spectral shift of AP in neat CO_2 is 70% of the maximum at 35 °C, and 55% at 45 °C. Considering equal contribution from each solvating molecule, these fractions represent the percentage occupation of a complete solvation sphere (more precisely speaking, the fraction of the interacting solvent molecules responsible for the spectral shift). In the mixtures, the reasoning is not so straightforward, but model free conclusions can be also derived. At $\rho_{CO_2} > 20$ M, half of the solvation sphere of AP is filled by ethanol when the concentration of this component is 0.025 M (see Fig. 3(b), middle curves). The correspondent data points are half way between the shifts in the pure two components. At this same concentration of ethanol and at the critical density of CO_2, the surrounding of AP is more ethanol like (65% at [EtOH]=0.025 M

and 90% at [EtOH]=0.125 M). This fact points to an additional coverage of the solvation sphere by ethanol, thus filling vacant positions and attaining a total solvent occupation exceeding the estimated 70% for neat CO_2. In all cases, at higher temperatures, entropic factors favor cluster dissociation.

Finally, Fig. 3 shows that the spectral shift in neat 10 M CO_2 is greater than in hexane by 600 cm^{-1} at 35 °C, and by 800 cm^{-1} at 45 °C. This can be explained taking into account that at this density most of the solvation shell is occupied by CO_2 and that CO_2 can interact with AP by quadrupole dipole stabilization, by Lewis acid–base interactions, as it does with water, and by H-bond acceptor interactions.

In spite of its simplicity and of the systematic deviations observed at the higher ethanol molar ratios, the model adopted in this analysis rendered meaningful conclusions regarding the occupation of the solvation sphere by solvents of very different affinity for the solute, and an explanation for the lack of entropic effects in the solvation compared to incompressible fluids.

Acknowledgements

References

[1] Thematic issue, Chem. Rev. 99 (1999) 353–634.
[2] G.E. Bennett, K. Johnston, J. Chem. Phys. 98 (1994) 441.
[3] Y.P. Sun, M.A. Fox, K. Johnston, J. Am. Chem. Soc. 114 (1992) 1187.
[4] J. Zhang, D.P. Roek, J.E. Chateauneuf, J.F. Brennecke, J. Am. Chem. Soc. 119 (1997) 9980.
[5] M. Khajehpour, J.F. Kauffman, J. Phys. Chem. A. 104 (2000) 9512.
[6] J.A. Hyatt, J. Org. Chem. 49 (1984) 5097.
[7] C.R. Yonker, S.L. Frye, D.R. Kolkworf, R.D. Smith, J. Chem. Phys. 90 (1986) 3022.
[8] M.E. Sigman, S.M. Lindley, J.E. Leffler, J. Am. Chem. Soc. 107 (1985) 1471.
[9] J.F. Kauffman, J. Phys. Chem. A. 105 (2001) 3433.
[10] J.E. Lewis, R. Biswas, A.G. Robinson, M. Maroncelli, J. Phys. Chem. B. 105 (2001) 3306.
[11] Y. Kimura, N. Hirota, J. Chem. Phys. 111 (1999) 5474.
[12] M.P. Heitz, M. Maroncelli, J. Chem. Phys. 101 (1997) 5852.
[13] C.B. Roberts, J. Zhang, J.E. Chateauneuf, J.F. Brennecke, J. Am. Chem. Soc. 115 (1993) 9576.
[14] J. Zagrobelny, T.A. Betts, F.V. Bright, J. Am. Chem. Soc. 115 (1993) 701.
[15] J.M. Tanko, R. Pacut, J. Am. Chem. Soc. 123 (2001) 5703.
[16] B. Fletcher, N. Kamrudin Suleman, J.M. Tanko, J. Am. Chem. Soc. 120 (1998) 11839.
[17] K.E. O' Shea, J.R. Combes, M.A. Fox, K. Johnston, Photochem. Photobiol. 54 (1991) 571.
[18] D. Andrew, B.T. Des Islet, A. Margaritis, A.C. Weedon, J. Am. Chem. Soc. 117 (1995) 6132.
[19] N.G. Bakhshiev, Y.T. Mazurenko, I.V. Piterskaya, Opt. Spectrosc. 21 (1966) 307.
[20] N.G. Bakhshiev, Opt. Spectrosc. 12 (1962) 309.
[21] W.R. Ware, S.K. Lee, G.J. Brant, P.P. Chow, J. Chem. Phys. 54 (1971) 4729.
[22] T. Harju, A.H. Huizer, C.A.G.O. Varma, Chem. Phys. 200 (1995) 215.
[23] E. Laitinen, K. Salonen, T. Harju, J. Chem. Phys. 105 (1996) 9771.
[24] T. Soujanya, T.S.R. Krishna, A. Samanta, J. Phys. Chem. 96 (1992) 8544.
[25] G. Saroja, A. Samanta, Chem. Phys. Lett. 246 (1995) 506.
[26] S. Das, A. Datta, K. Bhattacharyya, J. Phys. Chem. A. 101 (1997) 3299.
[27] A. Datta, S. Das, D. Mandal, K. Pal, K. Bhattacharyya, Langmuir 13 (1997) 6922.
[28] T.A. Betts, F.V. Bright, Appl. Spectrosc. 44 (1990) 1203.
[29] B.A. Pryor, P.M. Palmer, P.M. Andrews, M.B. Berger, T. Troxler, M.R. Topp, Chem. Phys. Lett. 271 (1997) 19.
[30] P.J. Suppan, J. Chem. Soc. Faraday Trans. I 83 (1987) 495.
[31] C.F. Chapman, R.S. Fee, M. Maroncelli, J. Phys. Chem. 99 (1995) 4811.
[32] D.E. Wetzler, C. Chesta, R. Fernández-Prini, P.F. Aramendía, J. Phys. Chem. A. 106 (2002) 2390.
[33] W. Rapp, H.H. Klingenberg, H.E. Lessing, Ber. Bunsenges. Phys. Chem. 75 (1971) 883.
[34] J.R. Lakowicz, Principles of Fluorescence Spectroscopy, second ed., Kluwer Academic, Plenum, NY, 1999 Chapter 7.
[35] P. Suppan, J. Photochem. Photobiol. A 50 (1990) 293.
[36] R.A. Moore, J. Lee, G.W. Robinson, J. Phys. Chem. 89 (1985) 3648.
[37] D. Yuan, R.G. Brown, J. Phys. Chem. A 101 (1997) 3461.
[38] S. Kim, K.P. Johnston, Ind. Eng. Chem. Res. 26 (1987) 1206.
[39] O. Kajimoto, Chem. Rev. 99 (1999) 355.
[40] J. Otomo, S. Koda, Chem Phys. 242 (1999) 241.
[41] S.A. Egorov, A. Yethiraj, J.L. Skinner, Chem. Phys. Lett. 317 (2000) 558.
[42] R. Fernández Prini, J. Phys. Chem. B 106 (2002) 3217.
[43] G. Sciaini, E. Marceca, R. Fernández Prini, Phys. Chem. Chem. Phys. 4 (2002) 3400.
[44] O. Kajimoto, M. Futakami, T. Kobayashi, K. Yamasaki, J. Phys. Chem. 92 (1988) 1347.
[45] D.E. Wetzler, P.F. Aramendía, M.L. Japas, R. Fernández-Prini, Int. J. Thermophys. 19 (1998) 27.
[46] J.F. Ely, J.W. Magee, W.M. Haynes, Research Report 110. Gas Proc. Assoc., 1987.
[47] G.S. Gurdial, N.R. Foster, S.L.J. Yun, K.D. Tilly, in: E. Kiran, J.F. Brennecke (Eds.), Supercritical Fluid Engineering Science, ACS, Washington, DC, 1993, p. 34.
[48] D.W. Jennings, M.T. Gude, A.S. Teja, in: E. Kiran, J.F. Brennecke (Eds.), Supercritical Fluid Engineering Science, ACS, Washington, DC, 1993, p. 10.
[49] K. Suzuki, H. Sue, M. Itou, R.L. Smith, H. Inomata, K. Arai, S. Saito, J. Chem. Eng. Data 35 (1990) 63.
[50] L.W. Flanagin, P.B. Balbuena, K.P. Johnston, P.J. Rossky, J. Phys. Chem. B 101 (1997) 7998.
[51] The free energy difference between relaxed excited and ground state for a solute with n solvent molecules in the solvation sphere ($\Delta F(n)_{00}$) and one with $n+1$ solvent molecules can be related to the rate constants for exit of one solvent molecule from the excited

state, k_{-e}, and from the ground state, k_{-g}, that are independent of occupation. If we take into account the cycle in Scheme 1 and the normal spectroscopic assumption that the 00 transition is half way between the maximum of the absorption and of emission, a constant spectral shift is derived: $1/2(\Delta F_{em}(n) - \Delta F_{em}(n+1)) = \Delta F(n)_{00} - \Delta F(n+1)_{00} = RT\ln(k_{-e}/k_{-g})$. This relation assumes that

the association rate constant, that depends on the diffusion in the bulk is equal for both electronic states of the solute.

[52] C. Reichardt, Chem. Rev. 94 (1994) 2319.
[53] Y. Marcus, Chem. Soc. Rev. 22 (1993) 409.
[54] T.G. Kim, M.F. Wolford, M.R. Topp, Photochem. Photobiol. Sci. 2 (2003) 576.